Jurnal Teknologi

Full Paper

THE EFFECTS OF ADDITIVE ON THE IMPACT ABSORPTION CAPABILITY OF MAGNETORHEOLOGICAL ELASTOMER

Normidatul Salwa Sobri, Khisbullah Hudha*, Zulkiffli Abd Kadir, Noor Hafizah Amer, Ku Zarina Ku Ahmad

Department of Mechanical Engineering, Universiti Pertahanan Nasional Malaysia, Kem Perdana Sungai Besi, 57000 Kuala Lumpur, Malaysia

Article history
Received
29 August 2022
Received in revised form
22 March 2023
Accepted
9 April 2023
Published Online
25 June 2023

*Corresponding author
k.hudha@upnm.edu.my

Graphical abstract

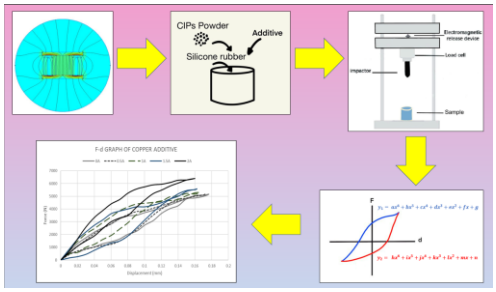

Abstract

Magnetorheological elastomer (MRE) is a smart material whose its damping and stiffness characteristics change when exposed to a magnetic field. MRE usually contains rubber and ferrous particles. Other materials such as additives, can improve physical properties of MRE during cyclic loading. However, limited research has been conducted into the effect of incorporating these additives on MRE performance when subjected to impact loading. Additives can change the MRE's structure such as stiffness and enhance its damping properties, especially its impact absorption capabilities. This study focuses on the force-displacement characteristics of additives and their relationships with MRE containing additives in impact absorption applications. This study uses ferrite, zinc, aluminum, and copper as additives in MREs fabrication and subjects the MREs to a drop impact test at varying applied currents of 0, 0.5, 1.0, 1.5, and 2.0 ampere. The experimental results show that the MRE containing ferrite has the highest average impact absorption capability of 2.24 Nm, followed by zinc, aluminum, and copper.

Keywords: Magnetorheological elastomer, additives, impact mitigation, varying current, impact absorption

Abstrak

Magnetorheological elastomer (MRE) adalah bahan pintar yang sifat fizikalnya berubah apabila terdedah kepada medan magnet. MRE biasanya mengandungi zarah getah dan besi. Bahan lain seperti bahan tambahan, dapat meningkatkan sifat fizikal MRE semasa beban kitaran. Walau bagaimanapun, penyelidikan yang telah dilakukan untuk memasukkan bahan tambahan ini pada prestasi MRE apabila mengalami beban impak sangat terhad. Bahan tambahan boleh mengubah struktur MRE seperti kekakuan dan meningkatkan sifat redamannya, terutamanya keupayaan penyerapan impak. Kajian ini memfokuskan pada ciri-ciri pemindahan daya bahan tambahan dan hubungannya dengan MRE yang mengandungi bahan tambahan dalam aplikasi penyerapan hentaman. Kajian ini menggunakan ferit, zink, aluminium, dan tembaga sebagai bahan tambahan dalam fabrikasi MRE dan menjalani ujian penjatuhan impak pada arus yang berbeza-beza 0, 0,5, 1,0, 1,5, dan 2,0 ampere. Hasil eksperimen menunjukkan bahawa MRE yang mengandungi ferit mempunyai purata keupayaan penyerapan hentaman tertinggi 2.24 Nm, diikuti oleh zink, aluminium, dan tembaga.

Kata kunci: Magnetorheological elastomer, aditif, mitigasi hentaman, variasi arus, penyerapan impak

1.0 INTRODUCTION

Of late, researchers have been investigating smart materials known as magnetorheological elastomers (MRE). MRE is a functional material whose mechanical characteristics can be dynamically modified by applying an external magnetic field to alter properties such as stiffness, frequency, and damping capability. As a result, MRE is used in many applications, especially vehicle absorbers and vibration mitigation. Additives enhance the properties of MRE under cyclic loading [1] by improving the ferrous particle alignment during the curing process.

Researchers have explored incorporating various additives in MRE, including silicone oil, multiwall carbon nanotube, and carbon black. Additives serve as base strengthener, vulcanizer, crosslinking agent, plasticizer, and accelerator. They also improve aging resistance, prevent the accumulation of magnetic particles and enhance the compatibility of the matrix material with the magnetic particles, thus improving the mechanical performance of MRE and its off-field and on-field properties. Figure 1 shows the schematic diagram of an MRE containing additives.

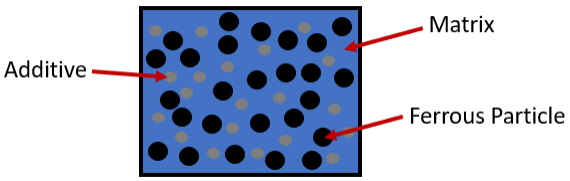

Figure 1 Schematic diagram of MRE

In early 2003, researchers evaluated [2] and improved [1], [3]–[6], common additives, such as mineral oils, phthalate esters, and silicone-based natural esters. According to [7], early research used plasticizers, carbon-based additives, and magnetic nanoparticles to produce MRE. In 2008, researchers investigated using reinforcement agents, such as carbon black (CB), carbon nanotubes (CNTs), and magnetic nanoparticles (MNPs) [5]. In terms of tear strength, carbon black (HAF N330) can increase the workability of rubber [8].

Furthermore, it is possible to modify the reinforcement agents to suit the desired MRE usage in different applications. For example, stearic acid acts as a lubricant that alters the rubber mechanism and improves the characteristics of the particle filler [9]. The frequently used additives in MRE formulation are zinc oxide (ZnO) and sulfur [10]–[12]. ZnO vulcanizes polychloroprene rubber, and it could also activate other rubbers. The proportion of ZnO is 3-5 per hundred resins (phr), where sulfur ranges from 0.1 to 5 phr [13].

An age resistor, or antioxidant, is a component of MRE that slows down the breakdown of the material and reduces the aging process in vulcanizates. The dosage of the antioxidants generally ranges between 1 and 3 phr [14]. Nanoflake Fe particles are used to produce MREs, where incorporating up to 6 wt.% nanoflake particles increased the magnetorheological (MR) effect (based on the loss factor) 1.56 times [15]. There is a suggestion that adding rod-shaped-ferrite (Fe_2O_3) nanoparticles to MREs could increase the MR effect.

Additionally, surface modification of Carbonyl Iron Particles (CIPs) is an emerging field for improving the properties of MREs [16]. The MREs fabricated using surface-modified CIPs have higher MR effects than pristine CIPs. It is crucial to determine the best additive material that enhances the MRE's mechanical properties, such as low damping ratio, good tensile strength, and high MR effect and impact absorption capability. Metal additives could improve the MRE properties by increasing the interfacial interactions between the fillers and matrices and polymer mobility [17].

Therefore, the ideal method for developing next generation MREs with better properties is to achieve optimum MRE morphology by combining the most appropriate matrix, ferrous particles, and additives. Even though many researchers have studied the methods for analyzing MREs, there are still unanswered questions about fabricating MREs with superior impact absorption capabilities. MRE is widely used in cyclic loading and vibration mitigation, including vibration isolators [18], [19] and dampers [20].

In shock attenuation application, it is essential to explore the potential of MRE in seismic mitigation [18], impact buffer [21], vehicle seat suspensions [22], and powertrain mount [23]. Kavlicoglu [24] explored the ways to soften the MRE mount in a variable weight system to reduce the degree of transmitted shock acceleration without bottoming out. Varying the MRE's stiffness allows the MRE mount to detect and mitigate shock and vibration events for various system weights.

The potential application of MRE with enhanced properties in impact loading has yet to be discovered. This study incorporated four additives in MRE, aluminum, copper, zinc, and ferrite. Aluminum is known for its high thermal conductivity, which makes it non-magnetic. Copper is malleable, ductile, non-magnetic, and a good conductor of heat and electricity. Zinc is diamagnetic and has a high heat capacity and heat conductivity. Ferrite is a magnetic material and has high magnetic permeability and electrical resistance.

This paper begins by introducing the MRE and additives. The second section focuses on the fabrication of MRE using additives. Section three describes the drop impact testing and presents the test results and a discussion. The last section concludes the study.

2.0 METHODOLOGY

The methodology of this study starts with the simulation of the magnetic field.

2.1 Simulation of The Magnetic Field Using Finite Element Magnetic Method

The Finite Element Magnetic Method (FEMM) is a programming language for solving low-frequency electromagnetic problems in two dimensions in the plane and axisymmetric domains. The model's initial simulation is required to determine the feasibility of further research. After simulating the magnetorheological elastomer model and getting significant results, more trial runs can be done to get a satisfactory and preliminary result before the actual work commences.

The finite element method has the significant advantage of being able to handle a wide range of geometries and nonhomogeneous materials without requiring changes to the computer code. Because the magnetorheological elastomer (MRE) contains magnetic filler, the magnetic problem was chosen. In the FEMM software, there are two subproblem options: planar problems and axisymmetric problems. Without the materials, the design is created with each node placed at point one to point four and the block label added as shown in Figure 2.

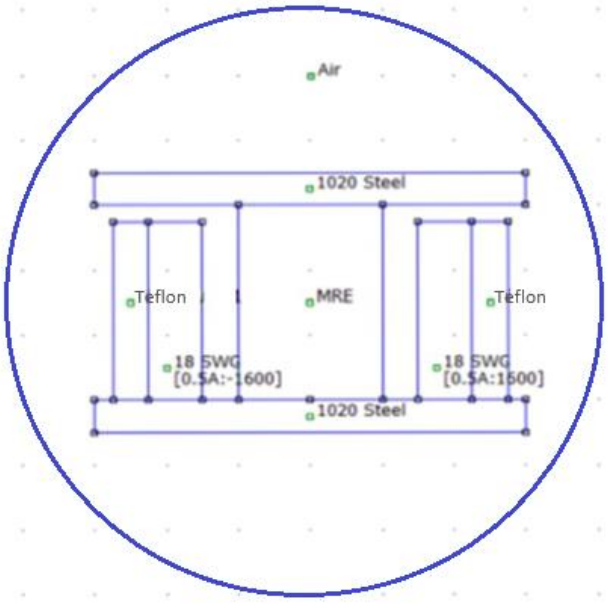

Figure 2 Schematic design diagram of the model

The planar problem was chosen because it expands along the plane's perpendicular axis and simplifies the flux density simulation. After determining the characteristics of the problem definition, nodes were created on the design, and at least two nodes had to be placed in the segments to connect them. The boundaries are formed in the desired shape for the design.

Each boundary area, including the white area outside the boundary, has a block label placed within it. Because of the variable nature of MRE materials, they are not available in the materials collection. To add the MRE to the design, the properties of the MRE are manually defined in the block property. The pattern of magnetic flux density is determined.

2.2 Fabrication of The MRE Containing Additives

The first step in fabricating the MRE is weighing all materials using a digital scale and the conventional method. The magnetic filler used for the MRE preparation is the 5-µm carbonyl iron particles (CIP) from Sigma Aldrich Chemistry. The matrices are room temperature vulcanization (RTV) silicone rubber from Craftiviti™ mixed with 60% CIP. The aluminum (Al) was from Bendosen, the zinc (Zn) and copper (Cu) from HmBG Chemicals, and Ferrite (Fe_2O_3) powder from AMC Group Limited. The magnetic additives were Ferrite and zinc, and the non-magnetic additives were aluminum and copper. Figure 3 explains the specimen preparation process. The process includes mixing, pouring, and curing stage.

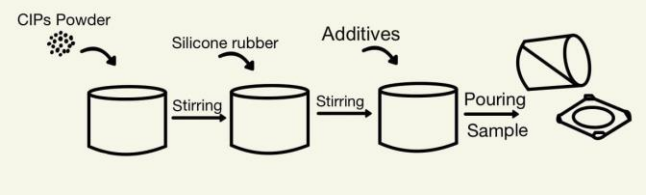

Figure 3 Fabrication process of the MRE

Table 1 lists the proportion of additives used in the MRE fabrication. The RTV silicone rubber and CIP are manually mixed in a container and gradually added the additives. After adding the hardener to the mixture, the mixture is poured into the mold for curing.

Table 1 Percentage of the additive in the MRE

Material	Percentage	Weight (g)
RTV silicone rubber	30%	9
Carbonyl iron powder	60%	18.9
Additive	10% of the CIP	1.89
Hardener	3% of the RTV SR	0.27

The curing takes up to 24 hours. Figure 4 shows the MRE in the mold during the curing. The release agent spray is used to facilitate the removal of the MRE from the mold. The MRE was then stacked between the metal plate on the strut device with an impactor and sleeve, ready to be tested.

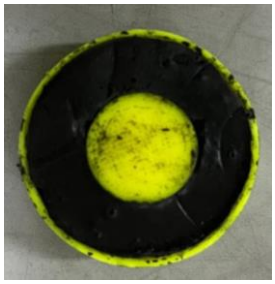

Figure 4 MRE in a mold during the curing process

2.3 Impact Testing of The MRE Containing Additive

This study performed a drop impact test on the MREs following the ASTM D2444 and ISO 3127 to determine the impact absorption capability. Generally, this test is conducted to determine the resistance of a material to a sudden external force. The drop impact test is also suitable for determining the impact resistance of thermoplastic pipes. This experiment used the Instron Drop Impact Machine and CEAST Software to set up the impact energy, impact velocity, falling height, tup holder mass, tup nominal mass, specimen support, and the applied current following the specifications in Table 2. The machine was set up in the Universiti Pertahanan Nasional Malaysia (UPNM) Automotive Lab.

Table 2 The parameter value of drop impact test

Parameter	Value
Impact energy	11 J
Impact velocity	2.00 m/s
Falling height	204 mm
Tup holder mass	4.3 kg
Tup nominal mass	1.2 kg
Specimen support	3 mm
Current	0.0A, 0.5A, 1.0A, 1.5A, 2.0A

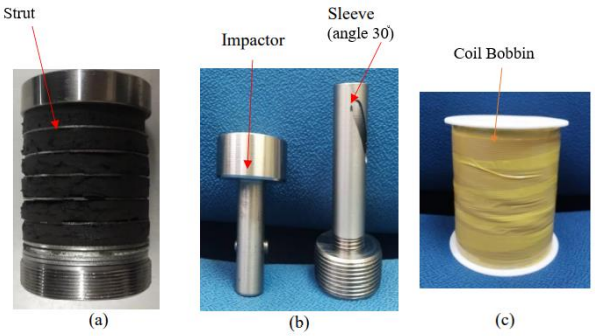

Figure 5 The MRE test device

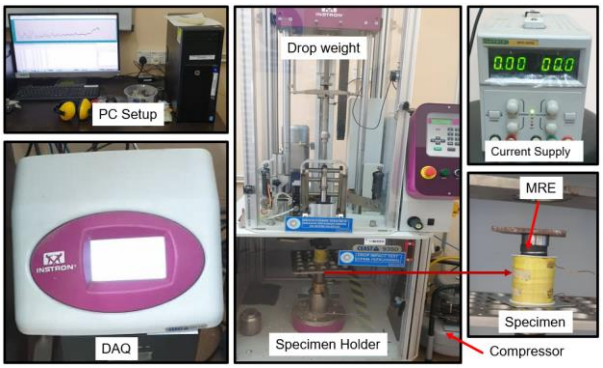

Figure 6 The setup for the drop impact test

Figure 5 shows the experimental setup. The cured MRE is layered between metal plates in Figure 5(a). Figure 5(b) and (c) shows the impactor and sleeve with 30° are used as actuator device in this experiment. The coil bobbin is used to generate magnetic field during the experiment. Figure 6 shows the experimental setup of the drop impact test. The experimental setup for drop impact test includes PC setup, Data Acquisition (DAQ), specimen holder and current supply. The experiments on each additive were performed at varying applied currents of 0A, 0.5A, 1.0A, 1.5A, and 2.0A. The specimen was housed in the MRE device specially designed to test the MRE properties. A hydraulic system pulled the impact weight to the release position before releasing it. The impact weight was fitted with an accelerometer and load cell to record the real-time acceleration and impact force.

This test is essential to assess the material behavior during the impact loading. The first step in the experiment was confirming the parameters of the drop impact loading. The impactor was set to the desired falling height and dropped onto the specimen within three seconds. The sensors recorded the data during the impact and sent it to the Data Acquisition (DAQ). The raw data in the experiment are time, displacement, and force.

3.0 RESULTS AND DISCUSSION

3.1 FEMM Simulation Result

The simulation results of the magnetic field using Finite Element Magnetic Method. Despite the various currents applied, the strength of the magnetic flux density in the magnetorheological elastomer is shown in descending order in the caption of the color area. Figures 7 and 8 show the flow density results for the MRE design at different currents of 0.5A, 1A, 1.5A, and 2A [25].

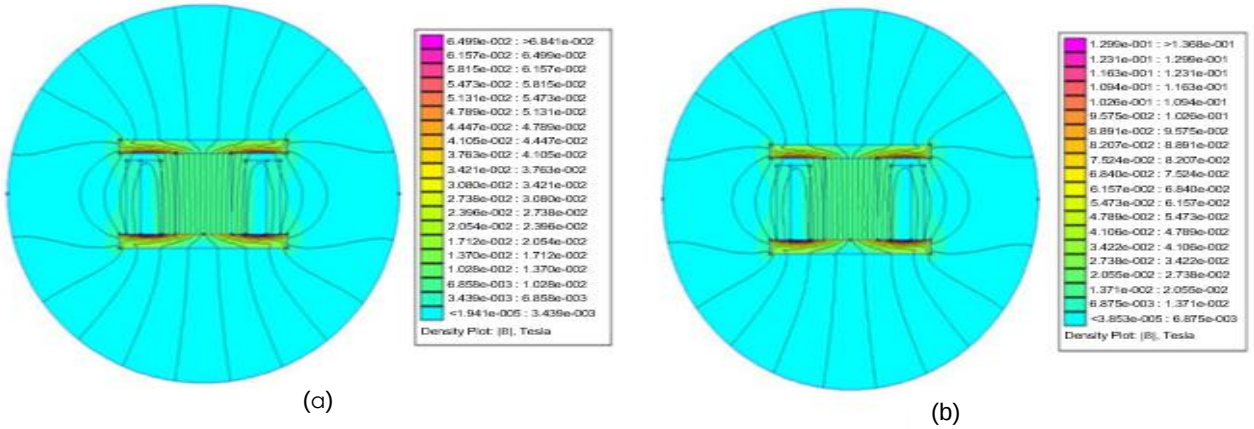

Figure 7 Flux density of MRE (a) 0.5 A, and (b) 1.0 A

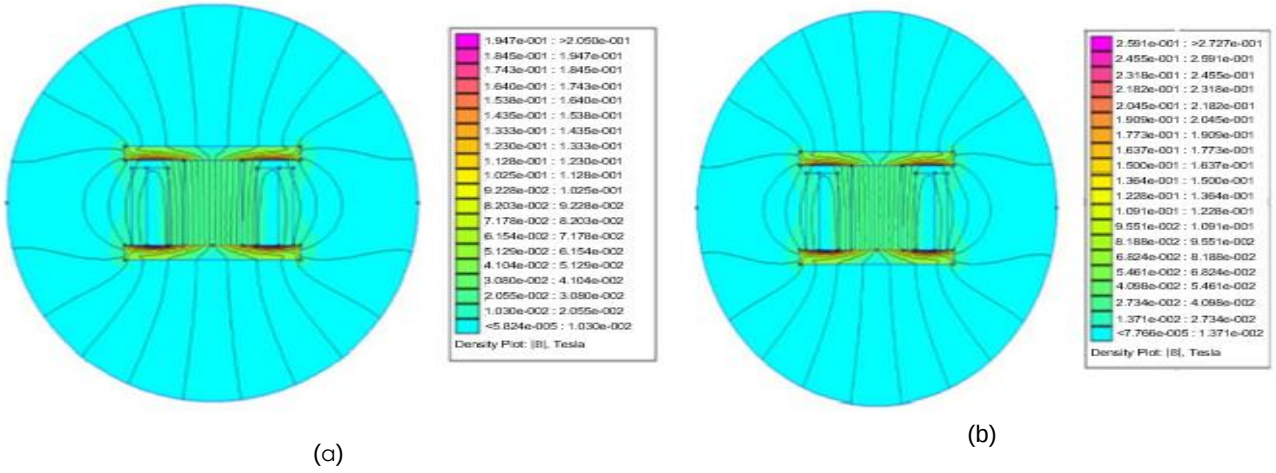

Figure 8 Flux density of MRE (a) 1.5 A, and (b) 2.0 A

As shown in Figures 7 and 8, the green zone in the MRE design has the lowest magnetic flux saturation. Meanwhile, the purple area in the MRE represents the highest magnetic flux saturation. Because magnetic coils connect the MRE's top and bottom halves, the magnetic flux is evenly distributed in both halves. As a non-magnetic conductor, Teflon covers the magnetic flux distributed by the MRE design. Because the magnetic waves flow evenly along the MRE, the carbonyl iron particle in the MRE composition is evenly aligned as a chain-like model.

To measure the dispersion of magnetic flux along with the MRE, the contour area is plotted from the center to the outer diameter of the MRE materials, which is one inch long. According to the magnetic flux density graph, MRE with a 0.5A current circuit emits the least magnetic flux, while MRE with a 2.0A current circuit emits the most. The bottom plate of the magnetic materials has a higher flux density value than the top plate because the MRE is directly placed on the base and top plates, and an air gap separates the coil.

Even though the top and bottom plates are different, the magnetic flux is most concentrated around the magnetic coil in mild steel. The magnetic flux is distributed evenly and uniformly, with no flux line distortion. Because the flow of flux around the system magnetizes the mild steel, the system changes into a magnetic circuit that can hold the MRE.

3.2 Drop Impact Testing Results

The MRE's Impact Absorption Capability (IAC) was calculated using the force-displacement (*F-d*) characteristics obtained through the experiment. The IAC is the area under the *F-d* graph. This study generated the polynomial functions of the sixth order from the *F-d* graph, where y_1 is the function of ascending line and y_2 is the function of descending line. Figure 9 shows an example of an *F-d* graph with functions.

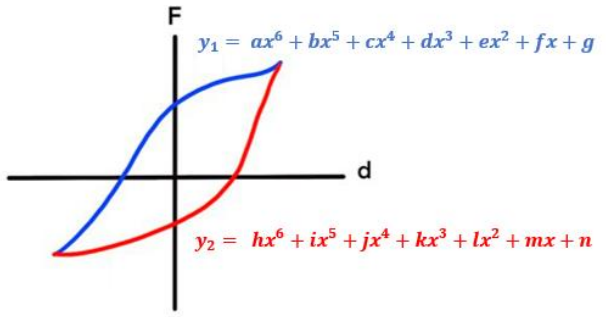

Figure 9 F-d graph with functions

Figure 9 shows that a, b, c, d, e, f, g, h, i, j, k, l, m, and n are constants, and x is the displacement. The functions were integrated to obtain the area under the F-d graph. Equation 3.1 is the formula for calculating the IAC.

$$IAC = \int_{x_{min}}^{x_{max}} (y_1 - y_2)\, dx \tag{3.1}$$

In Equation 3.1, x_{max} is the maximum displacement in the F-d graph, and x_{min} is the initial displacement. IAC is crucial in determining the most suitable additive for MRE, and its IAC calculation must be obtained from the F-d graph to acquire the energy or capability of the MRE. This method applies for calculating the IACs for the other additives and applied current. Tables 3, 4, 5, and 6 present the IAC, maximum displacement, force, and impact absorption capability values for MRE containing aluminum, copper, zinc, and ferrite, while Figures 10, 11, 12, and 13 show the F-d graphs for MRE containing aluminum, copper, zinc, and ferrite at varying applied currents.

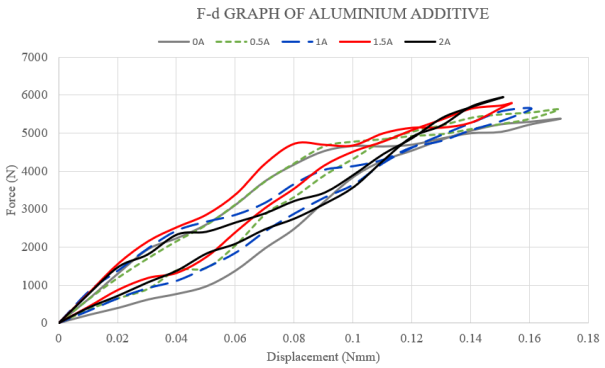

Figure 10 The F-d graph of the MRE with aluminum

Table 3 Maximum displacement, force, and IAC for MRE with aluminum

Current (A)	Max. Displacement (mm)	Max. Force (N)	IAC (Nm)
0	0.17	5387.87	1.51
0.5	0.17	5621.40	2.46
1	0.16	5654.76	0.38
1.5	0.15	5788.20	2.06
2	0.15	5955.01	0.81
Average	0.16	5681.45	1.44

Figure 10 shows the F-d trend when applying varying currents. The shape of the graph is related to a hysteresis loop where the compression and extension mode of MRE is represented. Table 3 shows that the current reduced displacement and increased the force. The IAC of each applied current can be calculated. Although the trend of IAC with increasing current fluctuates, the average of IAC of varying current will be calculated and compared to other additives. Aluminum is lightweight, durable, and a good conductor of heat and electricity (Wu *et al.*, 2021), making it a suitable additive for MRE. Moreover, the MRE containing aluminum has a higher impact absorption capability than the MRE with copper. Figure 11 shows that the F-d graph for MRE incorporated copper.

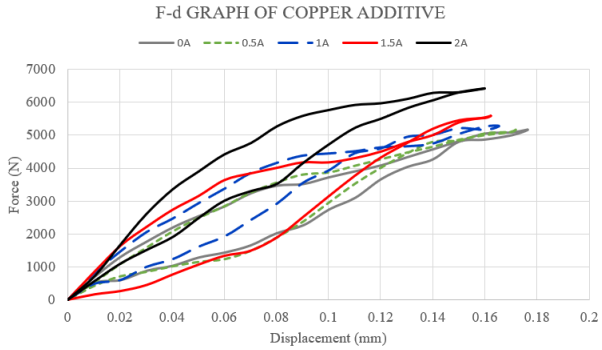

Figure 11 The F-d graph of the MRE with copper

Table 4 Maximum displacement, force, and IAC for MRE with copper

Current (A)	Max. Displacement (mm)	Max. Force (N)	IAC (Nm)
0	0.18	5171.02	0.27
0.5	0.17	5204.38	1.34
1	0.17	5287.78	3.66
1.5	0.16	5588.04	0.43
2	0.16	6405.39	0.67
Average	0.17	5531.32	1.26

Copper has excellent electrical and thermal conductivity. It influences the density of MRE (Jadhav *et al.*, 2020). However, unlike MRE incorporated with aluminum, the average maximum force and average IAC for the MRE-containing copper is lower. MRE incorporated with aluminum has the highest average IAC among non-magnetic additives. Figure 12 shows the F-d graph for MRE incorporated zinc.

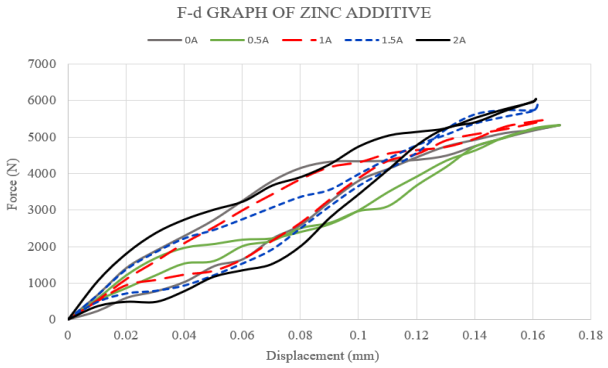

Figure 12 The F-d graph of the MRE with zinc

Table 5 Maximum displacement, force, and IAC for MRE with zinc

Current (A)	Max. Displacement (mm)	Max. Force (N)	IAC (Nm)
0	0.17	5321.15	1.65
0.5	0.17	5321.15	1.69
1	0.16	5471.27	2.71
1.5	0.16	5888.29	3.64
2	0.16	6038.42	0.85
Average	0.16	5608.06	2.11

Figure 12 shows the F-d graph for MRE incorporated with zinc, where higher applied current resulted in less displacement and higher maximum force. Zinc has a consistent quality, quick reaction time, and improves yields (Qi *et al.*, 2020). Zinc has a higher average IAC than aluminum and copper additives. Figure 13 shows the F-d graph of MRE incorporated Ferrite.

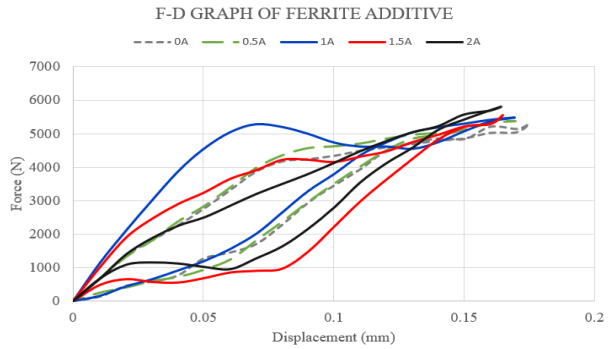

Figure 13 The F-d graph of the MRE with ferrite

Table 6 Maximum displacement, force, and IAC for MRE with ferrite

Current (A)	Max. Displacement (mm)	Max. Force (N)	IAC (Nm)
0	0.17	5287.78	0.67
0.5	0.17	5371.19	2.90
1	0.17	5487.95	0.78
1.5	0.16	5554.67	2.92
2	0.16	5804.89	3.91
Average	0.17	5501.30	2.24

The F-d graph for MRE incorporated with ferrite subjected to varying currents in Figure 13 has a broader leaf shape than the leaves for other additives. The MRE containing ferrite has the highest average IAC compared to other additives. Ferrite is ferromagnetic, which means it can be magnetized or is attracted to a magnet and is electrically non-conductive [26]. The low coercivity of ferrite makes it a suitable additive for MRE.

The F-d graph for each MRE incorporated additive has a different 'leaf' shape. For example, in Figure 13, the F-d graph shows that the MRE with a broader leaf-shaped F-d graph also has a higher impact absorption capability. However, the basic shape of the MRE F-d graph characteristics is a leaf, which represents the hysteresis behavior between compression and extension. The additive material did not change the properties of the F-d graph; it simply increased or decreased the magnitude of force. Tables 3, 4, 5, and 6 show that applying a 2 A current to MRE incorporated with ferrite resulted in the highest IAC, followed by a 1.5 A applied current to the MRE with zinc. The impact absorption capability of each MRE containing additive was calculated using the F-d graph, and the result is presented in Table 7.

Table 7 Total IAC for MRE incorporating additive

MRE incorporated additive	Average IAC (Nm)
MRE without additive	1.05
Aluminum	1.44
Copper	1.26
Ferrite	2.24
Zinc	2.11

Table 7 shows that MRE containing ferrite has the highest average impact absorption capability, followed by zinc, aluminum, copper, and MRE without additive. Ferrite is ferromagnetic materials, zinc is diamagnetic, while aluminum and copper are non-magnetic. MRE without additive has the lowest value of IAC compared to MRE incorporated with additives. Previous study from [27] also stated that MRE with additives will enhanced the physical

properties of MRE compared to MRE without MRE. The main difference between magnetic and non-magnetic materials is that magnetic materials are attracted to an external magnetic field because of their perfect magnetization alignment, and non-magnetic materials are pushed away from the external magnetic field due to their random magnetization pattern [28]. Because of this, the MRE added with ferrite has the best impact absorption capability.

4.0 CONCLUSION

This study fabricated MREs incorporated with aluminum, copper, zinc, and ferrite and tested each MRE using the drop impact test. The magnetic flux density was investigated to determine the model of the MRE. The experimental test sought to determine the impact absorption capability of the MREs subjected to varying applied currents using the force-displacement characteristics. The force increased with higher applied current, while the displacement decreased. The function for each MRE was generated using the experimental result and then used to calculate the impact absorption capability value. The MRE with ferrite has the highest average impact absorption capability of 2.24 Nm, followed by zinc (2.11 Nm), aluminum (1.44 Nm), and copper (1.27 Nm). The high impact absorption capability of the MRE with ferrite enhanced its properties, especially in impact mitigation applications. The force-displacement graph for ferrite has a broader leaf shape than the other additives.

Conflicts of Interest

The author(s) declare(s) that there is no conflict of interest regarding the publication of this paper.

Acknowledgement

This research is fully supported by FRGS grant, FRGS/1/2021/TK02/UPNM/02/1. The authors fully acknowledged Ministry of Higher Education (MOHE) and Universiti Pertahanan Nasional Malaysia for the approved fund which makes this important research viable and effective.

References

[1] M. H. A. Khairi *et al.* 2019. Role of Additives in Enhancing the Rheological Properties of Magnetorheological Solids: A Review. *Adv. Eng. Mater.* 21(3): 1-13. Doi: 10.1002/adem.201800696.

[2] A. Dargahi, R. Sedaghati, and S. Rakheja. 2019. On the Properties of Magnetorheological Elastomers in Shear Mode: Design, Fabrication and Characterization. *Compos. Part B Eng.* 159: 269-283. Doi: 10.1016/j.compositesb.2018.09.080.

[3] L. Ge, X. Gong, Y. Fan, and S. Xuan. 2013. Preparation and Mechanical Properties of the Magnetorheological Elastomer Based on Natural Rubber/Rosin Glycerin Hybrid Matrix. *Smart Mater. Struct.* 22(11). Doi: 10.1088/0964-1726/22/11/115029.

[4] J. E. Kim, J. Do Ko, Y. D. Liu, I. G. Kim, and H. J. Choi. 2012. Effect of Medium Oil on Magnetorheology of Soft Carbonyl Iron Particles. *IEEE Trans. Magn.* 48(11): 3442-3445. Doi: 10.1109/TMAG.2012.2195160.

[5] X. Song, W. Wang, F. Yang, G. Wang, and X. Rui. 2020. The Study of Enhancement of Magnetorheological Effect Based on Natural Rubber/Thermoplastic Elastomer SEBS Hybrid Matrix. *J. Intell. Mater. Syst. Struct.* 31(3): 339-348. Doi: 10.1177/1045389X19888790.

[6] Y. Kimura, S. Kanauchi, M. Kawai, T. Mitsumata, S. Tamesue, and T. Yamauchi. 2015. Effect of Plasticizer on the Magnetoelastic Behavior for Magnetic Polyurethane Elastomers. *Chem. Lett.* 44(2): 177-178. Doi: 10.1246/cl.140932.

[7] A. K. Bastola and M. Hossain. 2020. A Review on Magneto-Mechanical Characterizations of Magnetorheological Elastomers. *Compos. Part B Eng.* 200(May): 108348. Doi: 10.1016/j.compositesb.2020.108348.

[8] J. Fu, M. Yu, X. M. Dong, and L. X. Zhu. 2013. Magnetorheological Elastomer and Its Application on Impact Buffer. *J. Phys. Conf. Ser.* 412(1). Doi: 10.1088/1742-6596/412/1/012032.

[9] C. W. Lee, I. H. Kim, and H. J. Jung. 2018. Fabrication and Characterization of Natural Rubber-based Magnetorheological Elastomers at Large Strain for Base Isolators. *Shock Vib.* Doi: 10.1155/2018/7434536.

[10] X. Song, W. Wang, F. Yang, G. Wang, and X. Rui. 2018. Study on Dynamic Mechanical Properties of Magnetorheological Elastomers Based on Natural Rubber/Thermoplastic Elastomer Hybrid Matrix. *Nanotechnology*. 29(27).

[11] L. Xia, Z. Hu, and L. Sun. 2021. Micromechanics-based Simulation of Anisotropic Magneto-mechanical Properties of Magnetorheological Elastomers with Chained Microstructures. *Smart Mater. Struct.* 30(9). Doi: 10.1088/1361-665X/ac13b4.

[12] S. U. Khayam, M. Usman, M. A. Umer, and A. Rafique. 2020. Development and Characterization of a Novel Hybrid Magnetorheological Elastomer Incorporating Micro and Nano Size Iron Fillers. *Mater. Des.* 192. Doi: 10.1016/j.matdes.2020.108748.

[13] M. Maciejewska and A. Sowińska-Baranowska. 2022. The Synergistic Effect of Dibenzyldithiocarbamate Based Accelerator on the Vulcanization and Performance of the Silica-Filled Styrene–Butadiene Elastomer. *Materials*. 15(4): 1450. Doi: 10.3390/ma15041450.

[14] M. K. Shabdin *et al.* 2019. Material Characterizations of Gr-Based Magnetorheological Elastomer for Possible Sensor Applications: Rheological and Resistivity Properties. *Materials (Basel)*. 12(3): 1-15. Doi: 10.3390/ma12030391.

[15] C. J. Lee, S. H. Kwon, H. J. Choi, K. H. Chung, and J. H. Jung. 2018. Enhanced Magnetorheological Performance of Carbonyl Iron/Natural Rubber Composite Elastomer with Gamma-Ferrite Additive. *Colloid Polym. Sci.* 296(9): 1609-1613. Doi: 10.1007/s00396-018-4373-0.

[16] Y. Zhou *et al.* 2020. The Fabrication and Properties of Magnetorheological Elastomers Employing Bio-Inspired Dopamine Modified Carbonyl Iron Particles. *Smart Mater. Struct.* 29(5). Doi: 10.1088/1361-665X/ab785b.

[17] E. Burgaz and M. Goksuzoglu. 2020. Effects of Magnetic Particles and Carbon Black on Structure and Properties of Magnetorheological Elastomers. *Polym. Test.* 81(August): 106233. Doi: 10.1016/j.polymertesting.2019.106233.

[18] X. Gu, Y. Yu, Y. Li, J. Li, M. Askari, and B. Samali. 2019. Experimental Study of Semi-Active Magnetorheological Elastomer Base Isolation System Using Optimal Neuro Fuzzy Logic Control. *Mech. Syst. Signal Process.* 119: 380-398. Doi: 10.1016/j.ymssp.2018.10.001.

[19] A. Jalali, H. Dianati, M. Norouzi, H. Vatandoost, and M. Ghatee. 2020. A Novel Bi-Directional Shear Mode Magneto-Rheological Elastomer Vibration Isolator. *J. Intell. Mater. Syst. Struct*. 31(17): 2002-2019. Doi: 10.1177/1045389X20942314.

[20] K. Xiao, H. Bai, X. Xue, and Y. Wu. 2018. Damping Characteristics of Metal Rubber in the Pipeline Coating System. *Shock Vib.* 2018. Doi: 10.1155/2018/3974381.

[21] Ubaidillah, S. A. Mazlan, J. Sutrisno, and H. Zamzuri. 2014. Potential Applications of Magnetorheological Elastomers. *Appl. Mech. Mater*. 663: 695-699. Doi: 10.4028/www.scientific.net/AMM.663.695.

[22] P. Liu, X. Xia, N. Zhang, D. Ning, and M. Zheng. 2019. Torque Response Characteristics of a Controllable Electromagnetic Damper for Seat Suspension Vibration Control. *Mech. Syst. Signal Process.* 133: 106238. Doi: 10.1016/j.ymssp.2019.07.019.

[23] H. Zhou, H. Liu, P. Gao, and C. Le Xiang. 2018. Optimization Design and Performance Analysis of Vehicle Powertrain Mounting System. *Chinese J. Mech. Eng.* 31(2): Doi: 10.1186/s10033-018-0237-2.

[24] B. Kavlicoglu, Y. Liu, B. Wallis, H. Sahin, M. McKee, and F. Gordaninejad. 2020. Two-way Controllable Magnetorheological Elastomer Mount for Shock and Vibration Mitigation. *Smart Mater. Struct*. 29(2). Doi: 10.1088/1361-665X/ab4223.

[25] K. Hudha, N. Salwa Sobri, K. Sumasundram, N. Akmal Haniffah, Z. Abd Kadir, and M. Sabirin Rahmat. 2022. Investigation on the Effect of the Ferrous Particles Size on the Impact Absorption Capability of Magnetorheological Elastomer. *2022 IEEE 18th Int. Colloq. Signal Process. Appl. CSPA 2022 - Proceeding*. May: 299-303. Doi: 10.1109/CSPA55076.2022.9782010.

[26] G. Barrera *et al.*, "Cation Distribution Effect on Static and Dynamic Magnetic Properties of Co1-xZnxFe2O4 Ferrite Powders," *J. Magn. Magn. Mater.*, vol. 456, pp. 372–380, 2018, doi: 10.1016/j.jmmm.2018.02.072.

[27] S. A. A. Aziz *et al.* 2016. Effects of Multiwall Carbon Nanotubes on Viscoelastic Properties of Magnetorheological Elastomers. *Smart Mater. Struct.* 25(7). Doi: 10.1088/0964-1726/25/7/077001.

[28] O. N. Dubinin *et al.* 2022. Gradient Soft Magnetic Materials Produced by Additive Manufacturing from Non-Magnetic Powders. *J. Mater. Process. Technol.* 300(September): 117393. Doi: 10.1016/j.jmatprotec.2021.117393.